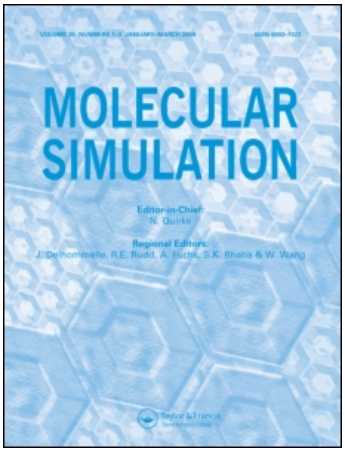

Molecular Simulation
Publication details, including instructions for authors and subscription information:
http://www.informaworld.com/smpp/title~content=t713644482

Adsorption of selected ions on the anatase TiO_2 (101) surface: a density-functional study

Marta Kinga Bruska[a]; Konrad Szaciłowski[bc]; Jacek Piechota[d]
[a] General Energy Research Department, Paul Scherrer Institut, Villigen, Switzerland [b] Department of Chemistry, Jagiellonian University, Kraków, Poland [c] Faculty of Non-Ferrous Metals, AGH University of Science and Technology, Kraków, Poland [d] Interdisciplinary Centre for Materials Modelling, University of Warsaw, Warszawa, Poland

To cite this Article Kinga Bruska, Marta , Szaciłowski, Konrad and Piechota, Jacek(2009) 'Adsorption of selected ions on the anatase TiO_2 (101) surface: a density-functional study', Molecular Simulation, 35: 7, 567 — 576
To link to this Article: DOI: 10.1080/08927020802654088
URL: http://dx.doi.org/10.1080/08927020802654088

Molecular Simulation
Vol. 35, No. 7, June 2009, 567–576

Taylor & Francis
Taylor & Francis Group

Adsorption of selected ions on the anatase TiO_2 (101) surface: a density-functional study

Marta Kinga Bruska[a], Konrad Szaciłowski[bc] and Jacek Piechota[d]*

[a]*General Energy Research Department, Paul Scherrer Institut, Villigen, Switzerland;* [b]*Department of Chemistry, Jagiellonian University, Kraków, Poland;* [c]*Faculty of Non-Ferrous Metals, AGH University of Science and Technology, Kraków, Poland;* [d]*Interdisciplinary Centre for Materials Modelling, University of Warsaw, Warszawa, Poland*

(*Received 31 October 2008; final version received 28 November 2008*)

Density-functional calculations of adsorption of the F^- and OH^- ions on the TiO_2 anatase (101) surface have been performed. Changes to the electronic properties prior to and after adsorption have been investigated. The most profound change in the electronic structure of the anatase surface after adsorption is the diminishing of the band gap of the system. While for the pure (without adsorbents) surface the band gap is 1.77 eV wide, for the modified surface with the F^- and OH^- ions the band gap widths equal to 0.35 and 0.39 eV, respectively. That means, the excitation energy after adsorption is over four times smaller than in the case of pure system. Nevertheless, in all the cases studied the anatase surface maintains its semiconducting properties.

Keywords: titanium dioxide; adsorption; electronic structure; density-functional theory

1. Introduction

Surface-modified semiconductors have found numerous applications as (photo)catalysts, chemosensors and biomimetic light-harvesting antennae. Recently, much attention has been focused on their capability of performing logic operations. The research in this field is stimulated by the natural limits of classical, silicon-based electronics. Various types of electronic interactions between the surface modification and the semiconducting support control yield photocurrent generated upon visible light irradiation and different efficiencies of the photosensitisation effect.

Among many materials studied, titanium dioxide, TiO_2, has been a subject of extensive research both experimentally (see for instance [1–25]) and theoretically [26–36] over the last decades. The main reason for such intense interest in TiO_2 is the wide range of its industrial applications and the expectation that insights into properties gained on the fundamental, atomic level will help to improve materials and device performance.

Most of the traditional applications of TiO_2 exploit its very large dielectric constant and refractive index. TiO_2 is commonly used as a dielectric in electronic devices [37,38] and as an optical coating: anti-reflection films, interference filters or optical wave guides [39,40]. It is widely used as a non-toxic white pigment in paints and cosmetic products [41], as corrosion-protective coatings and as a gas sensor [42–45]. It is also important in earth sciences, plays a role in the biocompatibility of bone implants [46] and in pure form it is used as a food additive [47]. Novel applications of TiO_2 are based on its surface and catalytic properties. Titanium dioxide is used in heterogeneous catalysis, electrochromic devices, as a photocatalyst, in solar cells for the production of hydrogen and electric energy [48]. The photoelectric and photochemical properties are especially interesting fields of research on TiO_2. Since about 1972, when Fujishima and Honda [11] published their work on the photolysis of water on TiO_2 electrodes without any external bias, titanium dioxide has continued to hold a dominant position in photocatalysis [49–53]. The latest research investigates titania usage for photo-assisted degradation of organic molecules due to its semiconducting properties. Applications of this process range from purification of wastewaters [49], disinfection [54], self-cleaning coatings [55] or protective coatings against environmental damage [56] to therapy against tumour cells [57–59]. Semiconducting metal oxides may change their photocatalytic properties upon adsorption of chemical compounds. The TiO_2-modified surfaces are another focus of active research [16–20]. The nanocrystallite structures, quantum dots as well as nanorods and nanotubes made from titanium dioxide [21–25] can significantly improve catalytic properties of this material and give another topic to study around TiO_2. The newest possible application of TiO_2 is connected with miniaturisation of electronic devices. Ultrathin titanium oxide films might be the gate material for replacing SiO_2 in MOSFET devices [60]. TiO_2 films doped with Co become ferromagnetic at room temperature. As they are optically transparent and semiconducting they may find application in spintronics

*Corresponding author. Email: jp@icm.edu.pl

ISSN 0892-7022 print/ISSN 1029-0435 online

DOI: 10.1080/08927020802654088
http://www.informaworld.com

[61]. It would be hard to find any other material with so many industrial applications and promising properties, especially photocatalytic ones, as TiO_2. It seems that the science of TiO_2 surface will play a key role in the future of high-tech industry. A comprehensive review of the properties of titanium dioxide surface has been given in [62].

Titanium dioxide occurs in nature as the well known naturally occurring minerals rutile, anatase and brookite, of which the first two are used commercially. The most common form is rutile, which is also the most stable form [63]. Anatase and brookite both convert to rutile upon heating [63]. Rutile, anatase and brookite all contain six coordinate titanium. However, some recent *ab initio* calculations show that anatase is more stable than rutile at 0 K [31–32]. Furthermore, anatase is more efficient than rutile for several applications, including photocatalysis [53], catalysis [64] and, especially, dye-sensitised solar cells [65,66]. In all these applications, surface properties are of major importance. However, while the surfaces of rutile have been extensively investigated [53,67], due to the limited availability of sufficiently large anatase single crystals, the fundamental surface properties of this polymorph are still largely unexplored. Only very recently, thanks to improved sample preparation techniques, have experimental studies of well-defined anatase surfaces started to appear [68,69].

Motivated by these advances, we have carried out an extensive first-principle investigation of the structure and energetics of the TiO_2 (101) anatase surface prior and after adsorption of the F^- and OH^- ions. The (101) surface is the most thermodynamically stable and the one mainly exposed in the TiO_2 anatase crystals [70]. It constitutes more than 94% of the crystal surface. To our best knowledge, this is the first report on the properties of the TiO_2 (101) anatase surface modified with the F^- and OH^- ions. However, the present work constitutes continuation of our earlier interest in *ab initio* modelling of oxide compounds [71–75].

The rest of the paper is organised as follows. Computational details are reported in Section 2. In Section 3, the geometrical considerations are presented and band structures with densities of states are analysed. In Section 4, the main points of this work are summarised and perspectives for future research are outlined.

2. Computational details

2.1 General settings

The calculations performed in this study were done using the VASP package [76] as implemented in MedeA environment (http://www.materialsdesign.com/). VASP evaluates the total energy of periodically repeated geometries, on the basis of density-functional theory (DFT) and the pseudopotential approximation. The electron–ion interaction is described by projected augmented waves [77,78]. Periodic boundary conditions are used, with the one-electron pseudo-orbitals expanded over a plane wave basis set. The expansion includes all plane waves whose kinetic energy is defined as $\hbar^2 k^2/2m < E_{\text{cut}}$, where k is the wave vector, m the electronic mass and E_{cut} the chosen cut-off energy. Calculations were performed using spin-unrestricted generalised gradient approximation (GGA) density-functional theory, which used Perdew–Burke–Emzerhof (PBE) exchange correlation functional [79]. All energies are extrapolated to a temperature of $T = 0$ K.

2.2 Settings for bulk TiO_2

Several tests have been initially performed to verify the accuracy of the method when applied to bulk TiO_2, as well as to clarify the different technical aspects of the calculations, such as the optimum pseudopotentials and sampling of the Brillouin zone.

For bulk rutile and anatase phases, using the energy cut-off of 550 eV and the k-spacing of 0.3 1/Å (corresponding to k-meshes of $8 \times 8 \times 8$ and $5 \times 5 \times 8$ for anatase and rutile, respectively) we have tested for convergence, using different sets of pseudopotentials and sampling schemes of the Brillouin zone. Calculations were performed with a standard set of pseudopotentials [76], but additional run was done with semi-core states pseudopotentials which treat 3s titanium states and higher ones as valence states, as well as with hard pseudopotentials for oxygen. Sampling of the Brillouin zone was performed using the Monkhorst–Pack scheme [80]. To minimise the errors in the Hellmann–Feynman forces due to the entropic contribution of the electronic free energy we have used as the integration scheme the Methfessel–Paxton technique [81] with a smearing of $\sigma = 0.2$ eV, as well as in another calculation tetrahedron with Blöchl correction technique [82]. In all cases, the total energy was converged to 10^{-5} eV. The changes in the accuracy of the final results were negligible, indicating that the convergence with respect to the basis set and k-spacing is ensured.

2.3 Settings for the TiO_2 (101) anatase surface

The TiO_2 (101) anatase surface is represented by a slab model with periodic boundary conditions applied in all three directions. Because the supercell (slab) representing the surface is much larger than the unit cell of bulk TiO_2, for the purpose of the present study the surface was modelled with less computationally demanding input parameters than those used in the calculations of the bulk. All the calculations were performed with standard set of pseudopotentials with a plane wave basis cut-off energy of 400 eV. Sampling of the Brillouin zone was performed using a Monkhorst–Pack scheme [80] with the k-mesh

of 2 × 2 × 1; the *k*-mesh was centred at the Γ-point of the Brillouin zone. The first-order Methfessel–Paxton smearing with a width of 0.2 eV was used as the integration scheme [82].

The slab used in computations contained 24 atoms, which build the first layer of the (101) anatase surface – see Figure 1(a) – with 10 Å of vacuum above the surface. Two different titanium sites with fivefold Ti(5)- and sixfold Ti(6)-coordinated titanium as well as twofold O(2) and threefold O(3)-coordinated oxygen can be distinguished at this surface. As electrophilic Ti(5) centres are easy accessible for adsorbents, they were preferably covered in the course of calculations. For the modified structures two of F^- (or respectively OH^-) ions were placed 2 Å above the Ti(5) centres and one oxygen vacancy was made to keep the system neutral in charge – see Figure 1(b) for the F^- adsorption and Figure 1(c) for the OH^- adsorption, respectively.

All the calculations have been performed for the non-relaxed cleaved crystal structure with the same bond distances as obtained in bulk calculations. One may claim that the slab used in computations is only a rough approximation to realistic description of the true system. However, the discrepancies introduced by insufficient size of the supercell are systematic, so that the main trends in the properties of modified surfaces can still be traced. The size reduction of the system under investigation was necessary to complete all the calculations in a reasonable time.

In order to report calculated results in a way consistent with other reports, we have applied following definitions and formulae. The surface energy is defined as:

$$E_{\text{surface}} = (E_{\text{slab}} - N{\cdot}E_{\text{bulk}})/A_{\text{surface}}, \qquad (1)$$

where E_{slab} is the total energy of the slab, N is the total number of TiO_2 units in the slab, E_{bulk} is the total energy of the TiO_2 unit in the bulk anatase phase, and A_{surface} is the total exposed area of the slab.

3. Results and discussion

3.1 *Bulk TiO_2*

Calculated lattice parameters of the rutile and anatase structures in comparison with results of neutron diffraction at the temperature of 15 K as listed in Ref. [6] are presented in Table 1. The calculated lattice parameters are in good agreement with the experimental values. The discrepancies are not higher than 1.6% over the experimental values for rutile and 1.0% for anatase, what is within the typical error of DFT in calculating the lattice constants of bulk materials. Note that these computed lattice parameters are generally overestimated with respect to experimental values, typical for the GGA approximation.

3.2 *Non-modified TiO_2 (101) anatase surface*

As mentioned above, the (101) anatase surface is the most thermodynamically stable and the one mainly exposed in the TiO_2 anatase crystals [70]. The distance between two

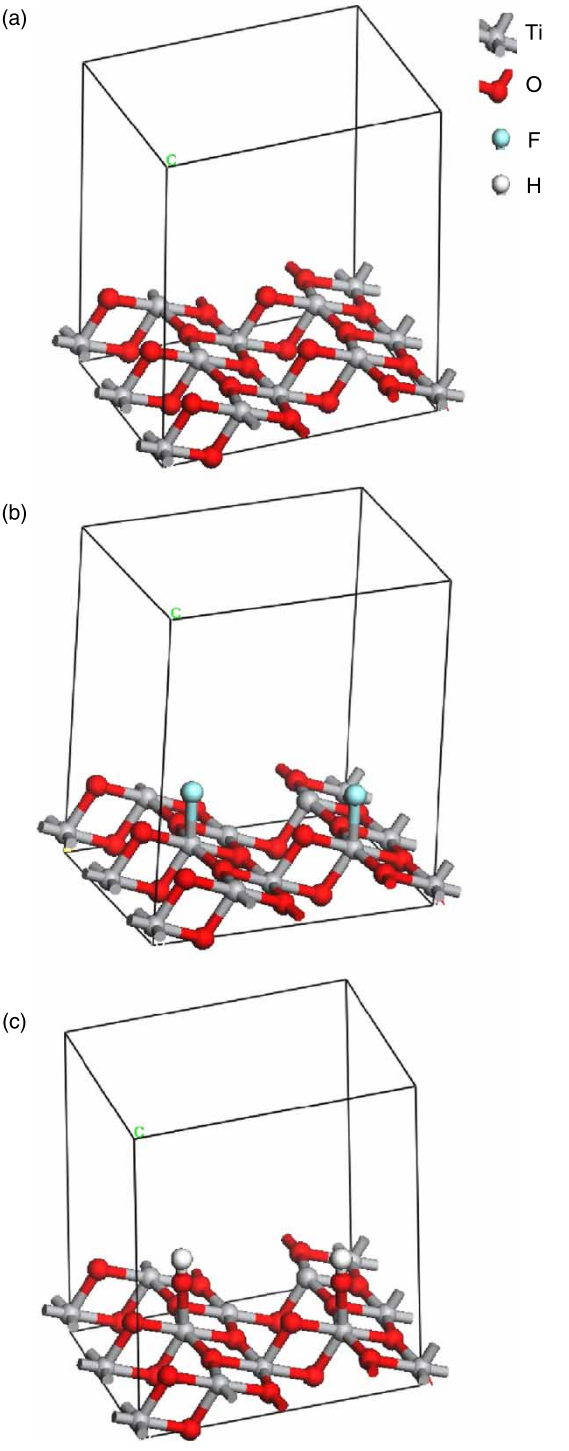

Figure 1. The structure of the stoichiometric TiO_2 anatase (101) surface. (a) Non-modified; (b) with F^- adsorbents; (c) with OH^- adsorbents.

Table 1. Lattice parameters in [Å] of the rutile and anatase TiO_2 structures.

Structure	Lattice parameter	Present work	Experiment[a]
Rutile	a	4.661	4.587
	c	2.969	2.954
	c/a	0.637	0.644
Anatase	a	3.822	3.782
	c	9.690	9.502
	c/a	2.535	2.535

[a] [6].

adjoining fivefold-coordinated titanium Ti(5) centres is 3.82 Å and the range between the neighbouring Ti(6) centres is 5.55 Å – see Figure 1. The calculated surface energy (Equation (1)) is 1.02 J/m^2, close to the energy of the unrelaxed anatase (101) surface of 1.28 J/m^2 computed by Lazzeri et al. [83].

Calculated band structure along the symmetry lines of the first Brillouin zone for anatase (101) surface is plotted in Figure 2(a), together with corresponding density of states (DOS) – see Figure 2(b). Partial DOS are shown in Figure 2(c)–(e). Zero in the energy scale corresponds to the Fermi level. The Fermi level is situated at the top of the valence band. This indicates the non-metallic properties of the material. The band gap is indirect, with the bottom of the conduction band at the Γ-point and the top of the valence band at the B-point. The width of this band gap equals 1.77 eV. However, the energy of the valence band at the Γ-point is only 0.25 eV lower than the top of the valence band. Thus, one can still think about the material as a direct band gap semiconductor. Similar to previously reported bulk calculations [30,31], the band gap is underestimated. The DFT approaches often fail to describe the experimental band gap for insulators and semiconductors. Another unphysical result from the calculation is the slightly negative DOS values for oxygen orbitals. This error can be attributed to the insufficient *k*-point sampling in the course of the computation. It can be considered as a numerical artefact and does not perturb general trends in the obtained results.

The valence electrons are distributed over two bands. The lower valence band lying just below −15.00 eV is 2.71 eV wide and contains mainly O 2s functions. The upper valence band is composed of the O 2p orbitals mixed with some contribution from Ti 3d functions and is 5.12 eV wide. The conduction band originates mainly from the Ti 3d orbitals, but one can find a small O 2p character as well. The hybridisation between O 2p and Ti 3d in both the conduction and upper valence bands indicates strong interactions between Ti and O atoms. As a result, the excitation across the band gap involves both the O 2p and Ti 3d states.

Integration of the total DOS up to the Fermi level gives the total number of electrons in the Ti 3d, Ti 4s, O 2p and O 2s orbitals in the supercell. As there are eight TiO_2 units in the supercell, the total number of electrons is equal to 128 as depicted in Figure 2(f).

3.3 *Modified surfaces*

3.3.1 *F^- adsorption*

Calculated band structure along the symmetry lines of the first Brillouin zone for anatase (101) surface with the F^- ions adsorbed is plotted in Figure 3(a), together with corresponding DOS – see Figure 3(b). Partial densities of states are shown in Figure 3(c)–(g).

In contrast to the non-modified surface, for the F^- adsorption the Fermi level is situated in the middle of the band gap. The predicted band gap is 0.35 eV wide. The valence electrons are distributed over three bands. The additional valence band, as compared to non-modified surface, is centred at −20.09 eV and originates from F 2s states. The subsequent band, as seen from the bottom of the band structure is 3.40 eV wide and corresponds to O 2s functions. The upper valence band is 5.90 eV wide and beside the O 2p orbitals and some contribution from Ti 3d functions contains the 2p orbitals from fluorine ions. The conduction band is still composed mainly of the Ti 3d orbitals with a small O 2p character, but in this case the band is splitted into two sub-bands. The interaction with fluorine energy levels is taking place here. The hybridisation between O 2p and Ti 3d is enriched with contribution coming from the fluorine orbitals in both the conduction and valence bands. There are interactions between F ions and Ti and O atoms. When the fluorine ions are adsorbed on the anatase surface the excitation across the band gap involves the O 2p, Ti 3d as well as F 2p states.

3.3.2 *OH^- adsorption*

Calculated band structure along the symmetry lines of the first Brillouin zone for anatase (101) surface with the OH^- ions adsorbed is plotted in Figure 4(a), together with corresponding (DOS) – see Figure 4(b). Partial densities of states are shown in Figure 4(c)–(g).

As for the F^- adsorption, for the OH^- adsorption the Fermi level is also situated in the middle of the band gap. The predicted band gap is 0.39 eV wide. The lowest valence band contains mainly O 2s functions. The upper valence band is composed of the O 2p orbitals and small contribution from Ti 3d functions. It is characterised by the highest width from all the presented systems, as its value equals to 6.09 eV. The conduction band is splitted into two sub-bands like in the system with the fluorine ions, but still it is composed mainly from the Ti 3d orbitals with a small contribution from the O 2p functions. As for the F^- adsorption one can see in this case the interaction of the TiO_2 slab levels with adsorbent orbitals. The hybridisation between O 2p and Ti 3d after adsorption is stronger than in

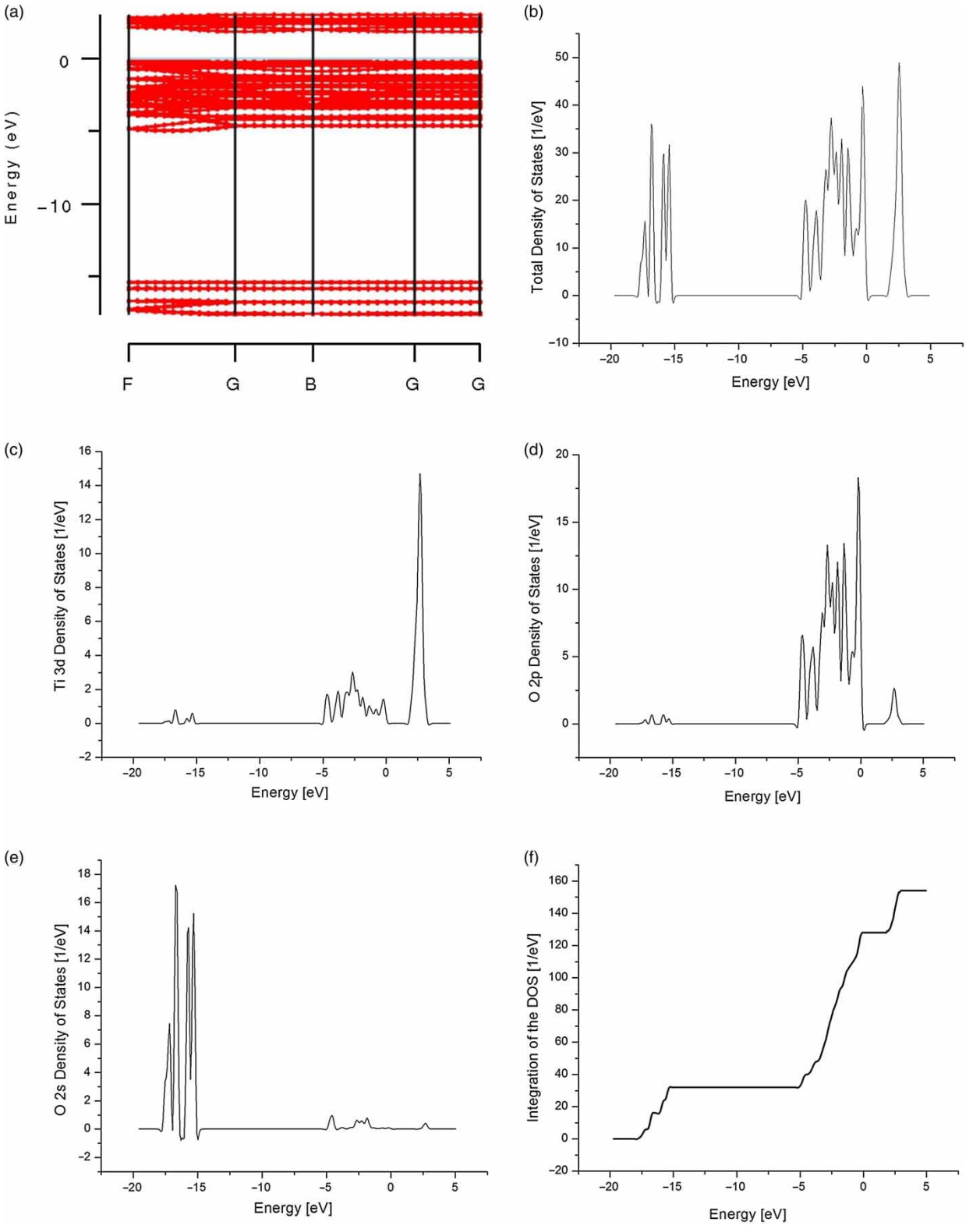

Figure 2. Electronic structure of the non-modified TiO_2 anatase (101) surface. (a) Band structure (G stands for Γpoint); (b) total DOS; (c) PDOS for Ti 3d orbitals; (d) PDOS for O 2p orbitals; (e) PDOS for O 2s orbitals; (f) Integrated total DOS.

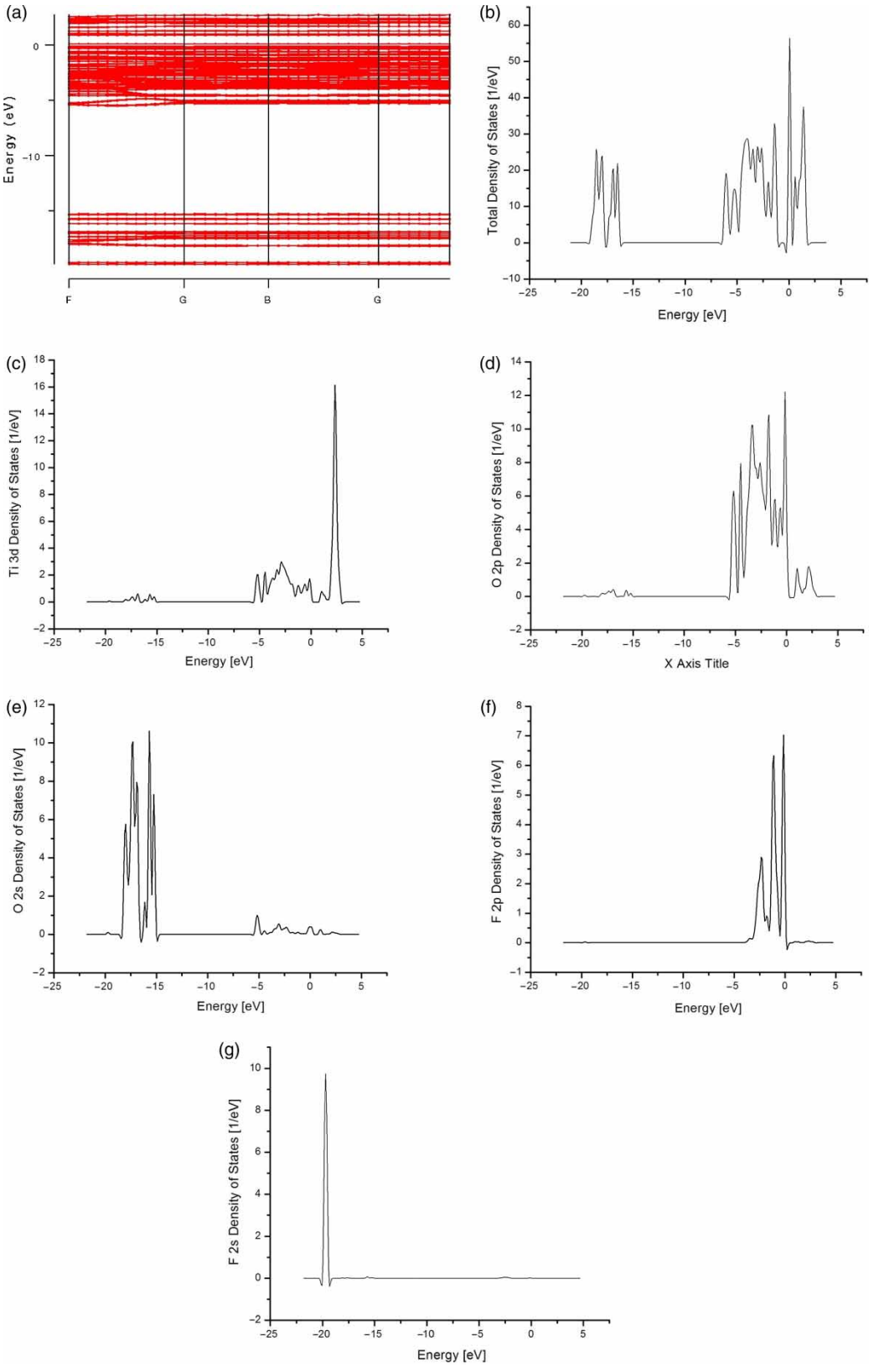

Figure 3. Electronic structure of the TiO_2 anatase (101) surface with F^- adsorbents. (a) Band structure (G stands for Γpoint); (b) total DOS; (c) PDOS for Ti 3d orbitals; (d) PDOS for O 2p orbitals; (e) PDOS for O 2s orbitals; (f) PDOS for F 2p orbitals; (g) PDOS for F 2s orbitals.

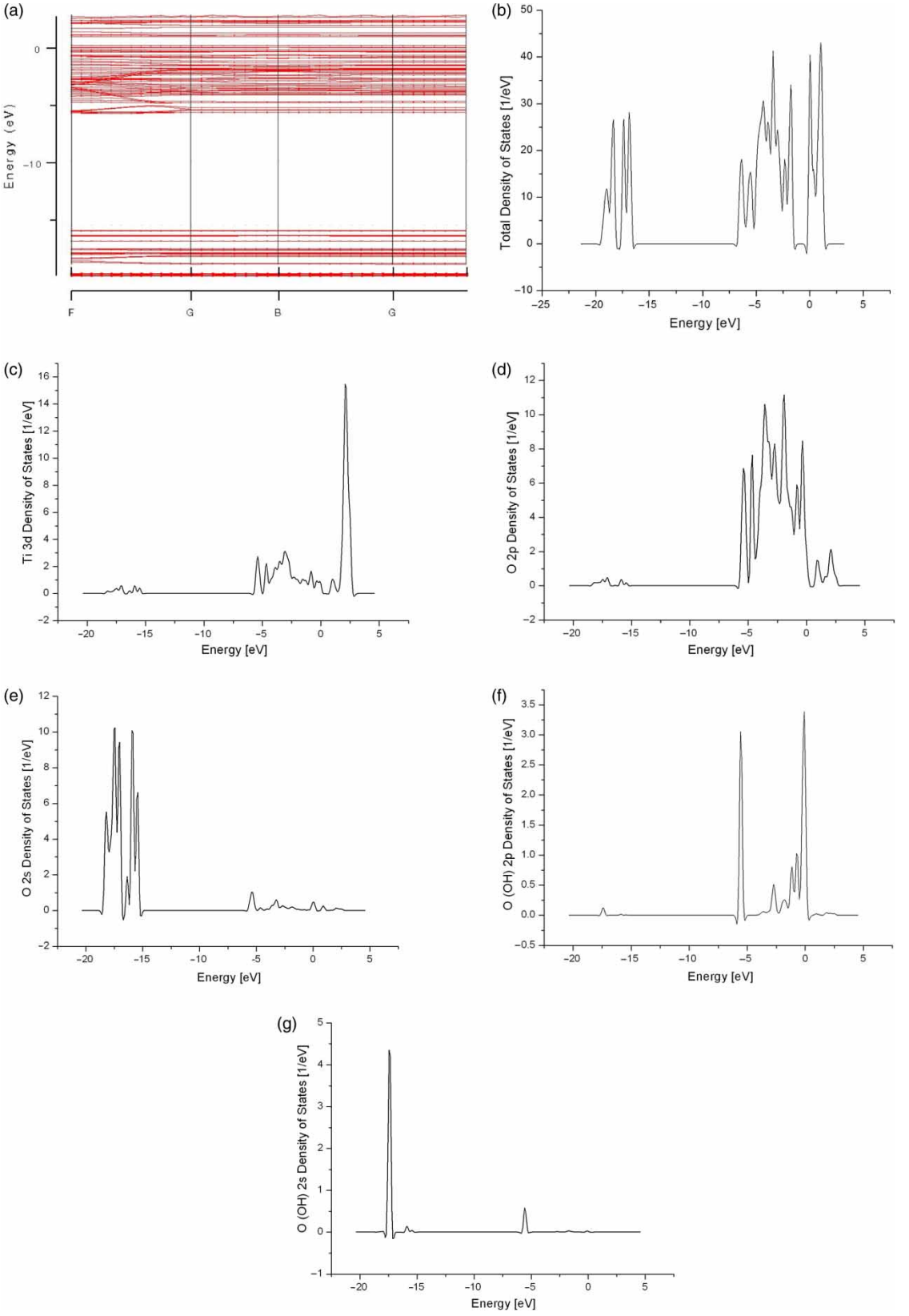

Figure 4. Electronic structure of the TiO_2 anatase (101) surface with OH^- adsorbents. (a) Band structure (G stands for Γpoint); (b) total DOS; (c) PDOS for Ti 3d orbitals; (d) PDOS for O 2p orbitals; (e) PDOS for O 2s orbitals; (f) PDOS for O (from OH groups) 2p orbitals; (g) PDOS for O (from OH groups) 2s orbitals.

the case of the non-modified surface. The OH^- ions enhance interactions of the O 2p and Ti 3d orbitals especially in the valence region. The excitation across the band gap involves the O 2p and Ti 3d states, but the O 2p orbitals are more important than they were in the model of the non-modified surface.

4. Summary and outlook

Band structures and densities of states were computed for unrelaxed non-modified TiO_2 (101) anatase surface and for anatase surfaces with the F^- and OH^- ions adsorbed. From decomposition of the total DOS into partial DOS, more detailed information about the ion–surface interactions was gained.

The most important change in the electronic structure of anatase surface after adsorption is the diminishing of the band gap. The excitation energy after adsorption is over four times lower. However, after adsorption the system still preserves its semiconducting properties. TiO_2 is a compound mostly ionic in character and hybridisation effects are not expected to be common in this case, especially in interaction with ions. This can be easily visible in the band structures which are flat in all the three cases studied. Some mixing of the O 2p and Ti 3d orbitals has occurred as well as small hybridisations of the ions and orbitals of the surface atoms (O 2p, Ti 3d and F 2p). As a result, the excitation across the band gap involves all states: O 2p, Ti 3d and F 2p when present.

To understand better the relevant photocatalytic properties of the modified anatase surfaces it is necessary to carry out more accurate computations. More precise results for DOS will permit a reasonable integration of the partial DOS that gives the total percentage of the given orbital that is occupied at a specified energy level. This provides information about electron transfer processes that is important for photocatalysis. The crystal orbital overlap populations from more accurate band structures are expected to give detailed information about bond formation.

The results obtained indicate that the systems under investigation constitute an interesting topic for further studies.

Note added in proofs

1. The authors would like to comment that although their calculations of adsorption of F^- and OH^- ions on the TiO_2 anatase (101) surface causes the diminishing of the band gap of the system after adsorption that is not reported in the experiment. It seems that F^- as well as OH^- ions adsorbed on the surface shift only the Fermi level, and additionally F^- ions generate the electrostatic barrier thus making interfacial electron transfer more difficult [16,84,85]. This may again suggest that standard supercells are too small to model the TiO_2 surface and apparently much larger supercells, especially containing higher number of Ti-O layers, should be used in the computations to recover the experimental results.

References

[1] D.T. Cromer and K. Herrington, *The structures of anatase and rutyle*, J. Am. Chem. Soc. 77 (1955), pp. 4708–4709.

[2] E.P. Meagher and G.A. Lager, *Polyhedral thermal expansion in the TiO_2 polymorphs: refinement of the crystal structures of rutile and brookite at high temperature*, Can. Mineral. 17 (1979), pp. 77–85.

[3] M. Horn, C.F. Schwerdtfeger, and E.P. Meagher, *Refinement of the structure of anatase at several temperatures*, Z. Kristallorg. 136 (1972), pp. 273–281.

[4] C. Abrahams and J.L. Bernstein, *Rutile: normal probability plot analysis and accurate measurement of crystal structure*, J. Chem. Phys. 55 (1971), pp. 3206–3211.

[5] Y. Kudoh and H. Takeda, *Single crystal X-ray diffraction study on the bond compressibility of fayalite, Fe_2SiO_4 and rutile, TiO_2 under high pressure*, Physica 139-140B (1986), pp. 333–336.

[6] J.K. Burdett, T. Hughbanks, J.G. Miller, J.W. Richardson, Jr., and J.V. Smith, *Structural-electronic relationships in inorganic solids: powder neutron diffraction studies of the rutile and anatase polymorphs of titanium dioxide at 15 and 295 K*, J. Am. Chem. Soc. 109 (1987), pp. 3636–3646.

[7] T. Restori, D. Schwarzenbach, and J.R. Schneider, *Charge density in rutile, TiO_2*, Acta Crystallogr. B 43 (1987), pp. 251–257.

[8] H. Shintani, S. Sato, and Y. Saito, *Electron-density distribution in rutile crystals*, Acta Crystallorgr. B 31 (1975), pp. 1981–1982.

[9] R. Brydson, B.G. Williams, W. Engel, H. Sauer, E. Zeitler, and J.M. Thomas, *Electron energy-loss spectroscopy (EELS) and the electronic structure of titanium dioxide*, Solid State Commun. 64 (1987), pp. 609–612.

[10] S.K. Sen, J. Riga, and J. Verbist, *2s and 2p X-ray photoelectron spectra of Ti^{4+} ion in TiO_2*, Chem. Phys. Lett. 39 (1976), pp. 560–564.

[11] A. Fujishima and K. Honda, *Electrochemical photolysis of water at a semiconductor electrode*, Nature 238 (1972), pp. 37–38.

[12] T. Watanabe, A. Nakajima, R. Wang, M. Minabe, S. Koizumi, A. Fujishima, and K. Hashimoto, *Photocatalytic activity and photoinduced hydrophilicity of titanium dioxide coated glass*, Thin Solid Films 351 (1999), pp. 260–263.

[13] A. Fujishima, T.N. Rao, and D.A. Tryk, *Titanium dioxide photocatalysis*, J. Photochem. Photobiol. C: Photochem. Rev. 1 (2000), pp. 1–21.

[14] T. Kemmitt, N.I. Al-Salim, M. Waterland, V.J. Kennedy, and A. Markwitz, *Photocatalyctic titania coatings*, Curr. Appl. Phys. 4 (2004), pp. 189–192.

[15] W. Zhang, T. Zhang, W. Yin, and G. Cao, *Relationship between photocatalytic activity and structure of TiO_2 thin film*, Chin. J. Chem. Phys. 20 (2007), pp. 95–98.

[16] A. Janczyk, E. Krakowska, G. Stochel, and W. Macyk, *Single oxygen photogeneration at surface modified titanium dioxide*, J. Am. Chem. Soc. 128 (2006), pp. 15574–15575.

[17] D. Mitoraj, A. Janczyk, M. Strus, H. Kisch, G. Stochel, P.B. Heczko, and W. Macyk, *Visible light inactivation of bacteria and fungi by modified titanium dioxide*, Photochem. Photobiol. Sci. 6 (2007), pp. 642–648.

[18] K. Szaciłowski, W. Macyk, M. Hebda, and G. Stochel, *Redox-controlled photosensitization of nanocrystalline titanium dioxide*, Chem. Phys. Chem. 7 (2006), pp. 2384–2391.

[19] K. Szaciłowski and W. Macyk, *Chemical switches and logic gates based on surface modified semiconductors*, C.R. Chimie 9 (2006), pp. 315–324.

[20] W. Macyk and H. Kisch, *Photosensitization of crystalline and amorphous titanium dioxide by platinum(IV) chloride surface complexes*, Chem. Eur. J. 7 (2001), pp. 1862–1867.

[21] E. Barborini, I.N. Kholmanov, P. Piseri, C. Ducati, C.E. Bottani, and P. Milani, *Engineering the nanocrystalline structure of TiO_2 films by aerodynamically filtered cluster deposition*, Appl. Phys. Lett. 81 (2002), pp. 3052–3054.

[22] J. Hong, J. Cao, J. Sun, H. Li, H. Chen, and M. Wang, *Electronic structure of titanium oxide nanotubules*, Chem. Phys. Lett. 380 (2003), pp. 366–371.

[23] D.V. Bavykin, E.V. Milsom, F. Marken, D.H. Kim, D.H. Marsh, D.J. Riley, F.C. Walsh, K.H. El-Abiary, and A.A. Lapkin, *A novel cation-binding TiO_2 nanotube substrate for electro- and bioelectrocatalysis*, Electrochem. Commun. 7 (2005), pp. 1050–1058.

[24] G.K. Mor, K. Shankar, M. Paulose, O.K. Varghese, and C.A. Grimes, *Use of highly-ordered TiO_2 nanotube arrays in dye-sensitized solar cells*, Nano Lett. 6 (2006), pp. 215–218.

[25] Z. Liu, X. Zhang, S. Nishimoto, M. Jin, D.A. Tryk, T. Murakami, and A. Fujishima, *Anatase TiO_2 nanoparticles on rutile TiO_2 nanorods: a heterogeneous nanostructure via layer-by-layer assembly*, Langmuir 23 (2007), pp. 10916–10919.

[26] N. Daude, C. Gout, and C. Jouanin, *Electronic band structure of titanium dioxide*, Phys. Rev. B 15 (1977), pp. 3229–3235.

[27] J.K. Burdett, *Electronic control of the geometry of rutile and related structures*, Inorg. Chem. 24 (1985), pp. 2244–2253.

[28] B. Silvi, N. Fourati, R. Nada, and C.R.A. Catlow, *Pseudopotential periodic Hartree–Fock study of rutile TiO_2*, J. Phys. Chem. Solids 52 (1991), pp. 1005–1009.

[29] A. Fahmi, C. Minot, B. Silvi, and M. Causa, *Theoretical analysis of the structures of titanium dioxide crystals*, Phys. Rev. B 47 (1993), pp. 11717–11724.

[30] S.-Di Mo and W.Y. Ching, *Electronic and optical properties of three phases of titanium dioxide: rutile, anatase, and brookite*, Phys. Rev. B 51 (1995), pp. 13023–13032.

[31] M. Mikami, S. Nakamura, O. Kitao, H. Arakowa, and X. Gonze, *First-principles study of titanium dioxide: rutile and anatase*, Jpn. J. Appl. Phys. 39 (2000), pp. L847–L850.

[32] J. Muscat, V. Swamy, and N.M. Harrison, *First-principles calculations of the phase stability of TiO_2*, Phys. Rev. B 65 (2002), pp. 224112-1–224112-15.

[33] K.M. Glassford and J.R. Chelikowsky, *Structural and electronic properties of titanium dioxide*, Phys. Rev. B 46 (1992), pp. 1284–1288.

[34] J.K. Dewhurst and J.E. Lowther, *High-pressure structural phases of titanium dioxide*, Phys. Rev. B 54 (1996), pp. R3673–R3675.

[35] Y. Zhang, W. Lin, Y. Li, K. Ding, and J. Li, *A theoretical study on the electronic structures of TiO_2: effect of Hartree–Fock exchange*, J. Phys. Chem. B 109 (2005), pp. 19270–19277.

[36] K.S. Jeong, Ch. Chang, E. Sedlmayr, and D. Sulzle, *Electronic structure investigation of neutral titanium oxide molecules Ti_xO_y*, J. Phys. B: At. Mol. Opt. Phys. 33 (2000), pp. 3417–3430.

[37] J.M. Wu and C.J. Chen, *Effect of powder characteristics on microstructures and dielectric properties of (Ba,Nb)-doped titania ceramics*, J. Am. Ceram. Soc. 73 (1990), pp. 420–424.

[38] W.D. Brown and W.W. Grannenmann, *C-V characteristics of metal-titanium dioxide-silicon capacitors*, Solid State Electron. 21 (1978), pp. 837–846.

[39] Y. Sawada and Y. Taga, *TiO_2/(indium tin oxide) multilayer film; a transparent IR reflector*, Thin Solid Films 116 (1984), pp. L55–L57.

[40] K.L. Siefering and G.L. Griffin, *Growth kinetics of CVD TiO_2: influence of carrier gas*, J. Electrochem. Soc. 137 (1990), pp. 1206–1208.

[41] G. Wakefield and J. Stott, *Photostabilization of organic UV-absorbing and anti-oxidant cosmetic components in formulations containing micronized manganese-doped titanium oxide*, J. Cosmet. Sci. 57 (2006), pp. 385–395.

[42] E.M. Logothetis and W.J. Kaiser, *TiO_2 film oxygen sensor made by chemical vapor deposition from organometallics*, Sens. Actuat. 4 (1983), pp. 333–340.

[43] B. Nicoloso, *TiO_2 and Bi_2O_3 thin film oxygen sensor materials*, Ber. Bunsenges. Phys. Chem. 94 (1990), pp. 731–737.

[44] K. Katayama, K. Hasegawa, Y. Takahashi, T. Akiba, and H. Yanagida, *Humidity sensitivity of Nb_2O_5-doped TiO_2 ceramics*, Sens. Actuat. A 24 (1990), pp. 55–60.

[45] H. Tang, K. Prasad, R. Sanjines, and F. Lévy, *TiO_2 anatase thin films as gas sensors*, Sens. Actuators B 26 (1995), pp. 71–75.

[46] F. Ahu Akin, H. Zreiqat, S. Jordan, M.B.J. Wijesundara, and L.Hanley, *Preparation and analysis of macroporous TiO_2 films on Ti surfaces for bone-tissue implants*, J. J. Biomed. Mater. Res. A 57 (2001), pp. 588–596.

[47] L.G. Phillips and D.M. Barbano, *The influence of fat substitutes based on protein and titanium dioxide on the sensory properties of lowfat milks*, J. Dairy Sci. 80 (1997), pp. 2726–2733.

[48] K. Rajeswar, *Materials aspects of photoelectrochemical energy-conversion*, J. Appl. Electrochem. 15 (1985), pp. 1–22.

[49] A. Mills, H.R. Davies, and D. Worsley, *Water purification by semiconductor photocatalysis*, Chem. Soc. Rev. 22 (1993), pp. 417–425.

[50] O. Legrini, E. Oliveros, and A.M. Braun, *Photochemical processes for water treatment*, Chem. Rev. 93 (1993), pp. 671–698.

[51] A. Heller, *Chemistry and applications of photocatalytic oxidation of thin organic films*, Acc. Chem. Res. 28 (1995), pp. 503–508.

[52] M. Hoffmann, S. Martin, W. Choi, and D. Bahnemann, *Environmental applications of semiconductor photocatalysis*, Chem. Rev. 95 (1995), pp. 69–86.

[53] A.L. Linsebigler, G. Lu, and J.T. Yates, *Photocatalysis on TiO_2 surfaces: principles, mechanisms, and selected results*, Chem. Rev. 95 (1995), pp. 735–758.

[54] P.-C. Maness, S. Smolinski, D.M. Blake, Z. Huang, E.J. Wolfrum, and W.A. Jacoby, *Bactericidal activity of photocatalytic TiO_2 reaction: toward an understanding of its killing mechanism*, Appl. Environ. Microbiol. 65 (1999), pp. 4094–4098.

[55] Y. Paz, Z. Luo, L. Rabenberg, and A. Heller, *Photooxidative self-cleaning transparent titanium dioxide films on glass*, J. Mater. Res. 10 (1995), pp. 2842–2848.

[56] I. Poulios, P. Spathis, A. Grigoriadou, K. Delidou, and P. Tsoumparis, *Protection of marbles against corrosion and microbial corrosion with TiO_2 coatings*, J. Environ. Sci. Health 34 (1999), pp. 1455–1472.

[57] R. Cai, K. Hashimoto, K. Itoh, Y. Kubota, and A. Fujishima, *Photokilling of malignant cells with ultrafine TiO_2 powder*, Bull. Chem. Soc. Jpn. 64 (1991), pp. 1268–1273.

[58] A. Fujishima, R. Cai, K. Hashimoto, H. Sakai, and Y. Kubota, *Photocatalytic purification and treatment of water and air*, in *Trace Metals and the Environment*, D.F. Ollis and H. Al-Ekabi, eds., Elsevier, New York, 1994, pp. 193–205.

[59] H. Sakai, R. Baba, K. Hashimoto, Y. Kubota, and A. Fujishima, *Selective killing of a single cancerous cell T24 with TiO_2 semiconducting microelectrode under irradiation*, Chem. Lett. 24 (1995), pp. 185–186.

[60] S.A. Campbell, H.-S. Kim, D.C. Gilmer, B. He, T. Ma, and W.L. Gladfelter, *Titanium dioxide (TiO_2)-based gate insulators,* IBM J. Res. Devlop. 43 (1999), pp. 383–392.

[61] Y. Matsumoto, T. Shono, T. Hasegawa, T. Fukumura, M. Kawasaki, P. Ahmet, T. Chikyow, S. Koshihara, and H. Koinuma, *Room temperature ferromagnetism in transparent transition metal-doped titanium dioxide*, Science 291 (2001), pp. 854–856.

[62] U. Diebold, *The surface science of titanium dioxide*, Surf. Sci. Rep. 48 (2003), pp. 53–229.

[63] N.N. Greenwood and A. Earnshaw, *Chemistry of the Elements*, 2nd ed., Butterworth-Heinemann, Oxford, 1997.

[64] K.I. Hadjiivanov and D.G. Klissurski, *Surface chemistry of titania (anatase) and titania-supported catalysts*, Chem. Soc. Rev. 25 (1996), pp. 61–65.

[65] B. O'Regan and M. Grätzel, *A low-cost, high-efficiency solar cell based on dye-sensitized colloidal TiO_2 films*, Nature 353 (1991), pp. 737–740.

[66] A. Hagfelt and M. Grätzel, *Light-induced redox reactions in nanocrystalline systems*, Chem. Rev. 95 (1995), pp. 49–68.

[67] H.J. Freund, *Oxide surfaces*, Faraday Discuss. 114 (1999), pp. 1–31.

[68] G.S. Herman, M.R. Sievers, and Y. Gao, *Structure determination of the two-domain (1×4) anatase TiO_2(001) Surface*, Phys. Rev. Lett. 84 (2000), pp. 3354–3357.

[69] R. Hengerer, P. Bolliger, M. Erbudak, and M. Grätzel, *Structure and stability of the anatase TiO_2 (101) and (001) surfaces*, Surf. Sci. 400 (2000), pp. 162–169.

[70] J. Ziółkowski, *New method of calculation of the surface enthalpy of solids*, Surf. Sci. 209 (1989), pp. 536–561.

[71] J. Piechota and M. Suffczyński, *Electronic structure of the CoO molecule*, Phys. Rev. A 48 (1993), pp. 2679–2685.

[72] J. Piechota and M. Suffczyński, *Density functional study of the diatomic first row transition metal oxides*, Z. Phys. Chem. 200 (1997), pp. 39–49.

[73] Z. Łodziana and J. Piechota, Ab initio *thermodynamic properties of point defects and O-vacancy diffusion in Mg spinels*, Phys. Rev. B 74 (2006), 184117.
[74] J. Wróbel and J. Piechota, *Structural properties of ZnO polymorphs*, Phys. Stat. Sol. B 244 (2007), pp. 1538. Erratum: Phys. Stat. Sol. B 244 (2007), pp. 4688–4690.
[75] J. Wróbel and J. Piechota, *On the structural stability of ZnO phases*, Solid State Commun. 146 (2008), pp. 324–329.
[76] G. Kresse and J. Furthmüller, *Efficient iterative schemes for* ab initio *total-energy calculations using a plane-wave basis set*, Phys. Rev. B 54 (1996), pp. 11169–11186.
[77] P.E. Blöchl, *Projector augmented-wave method*, Phys. Rev. B 50 (1994), pp. 17953–17979.
[78] G. Kresse and J. Joubert, *From ultrasoft pseudopotentials to the projector augmented-wave method*, Phys. Rev. B 59 (1999), pp. 1758–1775.
[79] J.P. Perdew, K. Burke, and M. Ernzerhof, *Generalized gradient approximation made simple*, Phys. Rev. Lett. 77 (1996), pp. 3865–3868.
[80] H.J. Monkhorst and J.D. Pack, *Special points for Brillouin-zone integrations*, Phys. Rev. B 13 (1976), pp. 5188–5192.
[81] M. Methfessel and A.T. Paxton, *High-precision sampling for Brillouin-zone integration in metals*, Phys. Rev. B 40 (1989), pp. 3616–3621.
[82] P.E. Blöchl, O. Jepsen, and O.K. Andersen, *Improved tetrahedron method for Brillouin-zone integrations*, Phys. Rev. B 49 (1994), pp. 16223–16233.
[83] M. Lazzeri, A. Vittadini, and A. Selloni, *Structure and energetics of stoichiometric TiO_2 anatase surfaces*, Phys. Rev. B 63 (2001), pp. 155409-1–155409-9.
[84] Ch.M. Wang and T.E. Mallouk, *Photoelectrochemistry and interfacial energetics of titanium dioxide photoelectrodes in fluoride-containing solutions*, J. Phys. Chem. 94 (1990), pp. 423–428.
[85] Ch.M. Wang and T.E. Mallouk, *Wide-range tuning of the titanium dioxide flat-band potential by adsorption of fluoride and hydrofluoric acid*, J. Phys. Chem. 94 (1990), pp. 4276–4280.